Cascading Failure Phenomenon in the Multi-Stage Hydraulically Fractured Wells

Non-peer reviewed manuscript submitted to Journal of Petroleum Science and Engineering

Konstantin Sinkov, Dimitry Chuprakov, Maxim Chertov, Dean Willberg, Pavel Spesivtsev

*Schlumberger Moscow Research, 13 Pudovkina st., Moscow, 119285, Russia**

(Dated: October 18, 2019)

Abstract

The phenomenon of cascading fracture failure during flowback and initial production from a horizontal multistage hydraulically fractured well is introduced, described, and investigated. First, a simplified analytical model of production from such well is built. This model allows evaluating a range of systems parameters through which the cascading failure evolves and performing a sensitivity study of this effect. Next, while keeping the physical model of the system relatively simple, the critical flow rates causing the motion of proppant pack in fractures are treated as random variables. This assumption brings the next level of sophistication to the model and allows demonstrating non-obvious effects. In particular, the well production rate losses due to cascading fracture failure are estimated. Finally, the proposed hypothesis is validated by conducting numerical simulations of flowback in the estimated conditions of cascading failure. As a practical outcome of this study, recommendations on the mitigation of the well productivity failure caused by cascading failure are formulated and discussed.

* P. Spesivtsev: pspesivtsev@slb.com

I. INTRODUCTION

Over the last decades, horizontal well drilling and multistage hydraulic fracturing have become increasingly popular in the oilfield industry. Typically, the combination of these technologies is required to produce oil and gas from low-permeability reservoirs at economic rates [4, 5, 15, 16]. Created fractures hydraulically connect the well to a reservoir and substantially increase well productivity roughly proportional to the total number of created fractures. In multistage fractured (MSF) wells, hydraulic fractures produce simultaneously from a reservoir to the same well and interact with each other via the shared fluid rate and bottom-hole pressure in the lateral. Such an interactive fracture behavior may lead to interesting and, at a first glance, unexpected results, such as emergent behavior and cascading fracture failure. Similarly to [18], we define this phenomena as follows. A cascading failure is a process in a system of interconnected hydraulic fractures in which the failure of one or few fractures triggers the failure of other fractures and so on.

Cascading processes are well-known in many branches of physics. For example, cascading outage processes in power systems have been reported and investigated [2, 7, 13]. To the best of our knowledge, such phenomena in producing MSF wells have not been reported in open literature. However, there are private observations and speculations among oil and gas field professionals about the possibility of cascading fracture failure in such wells. Therefore, the objective of this paper is to investigate the interactive fracture behavior in MSF wells and mechanisms leading to their possible cascading failure.

Key Questions

As mentioned above, the effect of cascading fracture failure lacks description in the open oilfield industry literature. Hence, throughout this work we are aiming at addressing the following four fundamental questions:

1. What is cascading fracture failure?
2. Why does it evolve in horizontal multistage fractured wells?
3. Where and under which conditions does it occur, and where does it not occur?
4. How can we avoid this negative event?

Cascading Fracture Failure Process

Cascading failure of fractures in an MSF well is the uncontrolled sequential productivity damage by flow of many fractures, such that failure of the first fracture causes subsequent failure of other fractures in the well. Suppose that all producing fractures are damageable. We assume that these fractures might fail if one of the parameters (e.g., pressure or rate) exceeds certain value. In this paper, we refer to this parameter as critical (critical pressure or critical rate). For example, the fractures might have different critical flow rate, below which they can produce without fracture damage. After the flow rate exceeds this value, the fracture fails and stops producing fluid to the well. Such situation may occur, for example, as a result of destabilization and washing out of the proppant from the near-wellbore region of this fracture. Under the high confining rock stress, the near-wellbore region unsupported by proppant will completely close and reduce fracture productivity to zero [10].

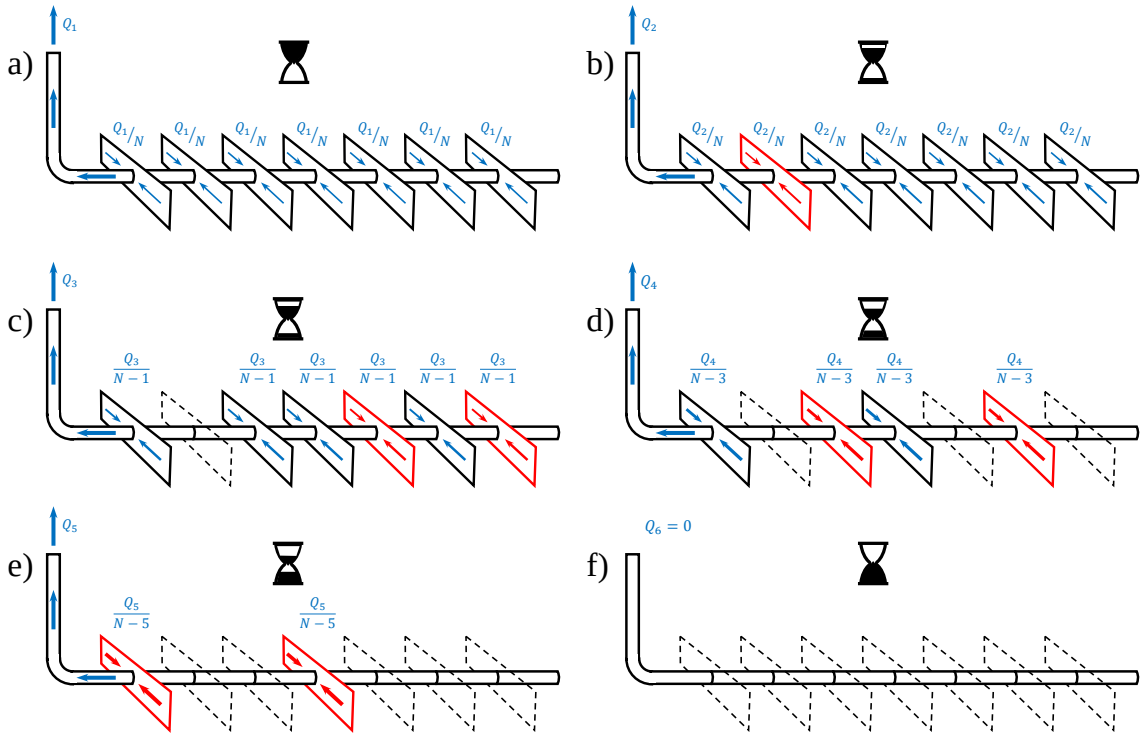

FIG. 1. Illustration of cascading fracture failure process.

Consider a completed horizontal well equipped with a choke at surface and having multiple

productive fractures created downhole. The mechanics of the cascading fracture failure process can be illustrated using the scenario presented in Fig. 1. The wellhead choke allows controlling the total production rate from the well. The fractures are different, so the critical parameter of failure is described by some distribution so that there is a varied failure resistance across the created fractures. The flow rate of fractures is induced by the pressure drop in the well with respect to the reservoir fluid pressure, also referred to as drawdown. Let us assume that initially (Fig. 1,a) the surface choke is set in such a way that the well produces at a relatively small production rate Q_1. This total production rate Q_1 is the sum of contributions from N hydraulic fractures, which produce with the same flow rate Q_1/N. At this rate, all fractures produce without any damage. Later, the choke is opened more, and the production rate is increased to Q_2 (Fig. 1,b). After this change, the weakest fracture in the well is damaged and stops producing (Fig. 1,c). Due to the presence of a wellhead choke, the total flow rate decrease is translated into the decrease of the bottomhole pressure and increase of the drawdown. This mechanism increases the flow rate bringing it to the value Q_3 that gets close to Q_2. Due to the smaller number of producing fractures, it increases the producing rate at each remaining fracture, which becomes $Q_3/(N-1) > Q_2/N$ (Fig. 1,c). As a result of the production rate per active fracture ramping up, the critical flow rate is reached for two other fractures in the well (red arrows in Fig. 1,c). As the choke opening increases, the well production rate continues increase leading in turn to increased drawdown for these fractures (Fig. 1,d). Following this fracture, other fractures continue to fail one by one (Fig. 1,e,f). This process of cascading failure may impact either some of the fractures or all of them, so that in extreme cases the entire well productivity could be lost (Fig. 1,f).

In this work, we investigate mechanics of interactive fracture behavior in a horizontal well during flowback and initial production. We evaluate conditions for triggering cascading fracture failure. The content of this paper is organized as follows. First, we explain the essence of the cascading fracture failure phenomenon in MSF horizontal wells using simple illustrations. Next, we build a physically justified analytical model of well production enabled by a large set of productive but damageable fractures. This deterministic model allows predicting onset of cascading fracture failure for the given well, wellhead, fracture, and reservoir parameters. Next, we introduce probabilistic description of the MSF well. Using this description, we perform comprehensive study of the full system behavior and discuss

implications of cascading failure events for the potential total loss of production. After this, we verify our analytical models by running accurate numerical simulations of flowback with consequent cascading failure using a rigorous numerical solver.

II. BASIC PHYSICAL MODEL

Consider an L-shaped well with N hydraulic fractures connected to its horizontal section and a choke at the wellhead (Fig.1). Assume that hydraulic fractures produce incompressible single-phase fluid at certain rates, depending on pressure drawdown. Because during initial production primarily water-like fluid is flowing back, the single-phase flow assumption can be justified. Individual fractures inflows q^k are commingled into the total production rate at the wellhead and the choke:

$$Q = \sum_{k=1}^{N} q^k. \tag{1}$$

Under such assumptions, the relation between the total mass flow rate Q and the pressure drop across choke $\Delta p_{ch} = p_{wh} - p_{whdc}$ is given by (see, for example, [12])

$$Q = KC^{-1/2}\sqrt{\Delta p_{ch}}, \quad K = \sqrt{2C_d^2 \rho A^2}, \quad C = \left(\left(\frac{d}{d_{ch}}\right)^4 - 1\right). \tag{2}$$

Here p_{wh} is the wellhead pressure, p_{whdc} is the wellhead downstream choke pressure, d_{ch} is the choke opening, d is the pipe diameter, $A = \pi d^2/4$ is the pipe cross-section area, and ρ is the liquid density. Discharge coefficient C_d describing irreversible friction losses is introduced into (2) empirically. Factor $C \in [0, \infty]$ represents operational conditions at the choke defined by the chosen management strategy; $C = 0$ corresponds to the fully open choke and $C = \infty$ corresponds to the fully closed choke.

Pressure drop in the wellbore is assumed to be dominated by the hydrostatic term. Accordingly, the bottomhole pressure p_{bh} is shared between all fractures and given by the sum of the wellhead pressure p_{wh} and the pressure drop at the vertical section of the well:

$$p_{bh} = p_{wh} + \rho g h. \tag{3}$$

Here g is the gravity acceleration and h is the depth of the horizontal well section relative to the wellhead.

The inflow from the k-th fracture is

$$q_k = J_k \left[p_{\text{res}} - p_{\text{bh}} \right], \tag{4}$$

where J_k is the productivity index of the fracture, which can be estimated, for example, using the Carter model [6].

An aggressive flowback strategy, when drawdown pressures and flow rates are high, can result in fracture damage. As mentioned above, the fracture conductivity can be damaged by different mechanisms that include, for example, washing of proppant out of the fracture, proppant crushing and embedment, fines migration, and tensile failure of rock and fracture faces. In this model, we assume that the k-th fracture maintains productivity as long as its rate is below some critical value, q_c^k or as long as the bottomhole pressure is above some critical value, p_c^k. Then, fractures can experience complete and irreversible loss of productivity if the failure criterion is met:

$$q^k > q_c^k. \tag{5}$$

or, in terms of pressure

$$p^k < p_c^k. \tag{6}$$

III. PROBABILISTIC DESCRIPTION

The merit of probabilistic description is that it is not necessary to specify the exact properties of individual fractures. A modern multistage hydraulically fractured well can be connected with over a hundred hydraulic fractures, and it can be impractical to characterize parameters of every fracture by either measurements or simulations or using a data analytics approach. Instead, it can be more convenient to specify probabilities of some parameters to stay within certain ranges established statistically. Such probabilistic description allows deriving response of the large system of hydraulically interacting fractures in terms of expected values and variances of parameters.

To formulate the probabilistic description, it is convenient to further simplify physical model described in section II. Productivity indices of all fractures are assumed to be the same, $J_k = J_0, \forall k$. Probabilistic analysis is performed during relatively short time interval, such that productivity index J_0 is assumed to be constant despite the $\sqrt{t}$ dependency typically

observed in the fracture productivity behavior [6]. Assume also that the bottomhole pressure is a non-increasing function of time. Each fracture is considered to operate with the constant productivity index J_0 if its individual rate q^k is less than some critical value q_c^k and totally and irreversibly lose productivity if q^k at some moment of time exceeds q_c^k.

Under these assumptions, the inflows are modeled by the following relation:

$$q^k = J_0\theta(p_{bh} - p_c^k)(p_R - p_{bh}). \tag{7}$$

Here $\theta(\cdot)$ is the Heaviside step function and $p_c^k = p_R - q_c^k/J_0$ is the critical bottomhole pressure for fracture failure.

Using equations (2) and (7), one can obtain the following system of algebraic equations describing steady states of the well:

$$\begin{gathered} Q = J_0(p_R - p_{bh})\sum_{k=1}^{N}\theta(p_{bh} - p_c^k), \\ Q = KC^{-1/2}\sqrt{p_{bh} - p_{bh0}}. \end{gathered} \tag{8}$$

It is important to note that during flowback the well is certainly not in steady state regime so that different transient effects (e.g. pressure and rate jumps) can take place as a result of changes in boundary conditions (e.g. changes of choke opening or pressure at the wellhead). These effects can also have impact on the evolution of cascading failure process. Nevertheless, in this work we consider these transient effects as the next order approximation to the considered problem. We demonstrate that cascading failure can be described and investigated using this steady-state formulation.

Here $p_{bh0} = p_{whdc} + \rho g h$ is the bottomhole pressure for the fully opened choke and $Q = \sum_{k=1}^{N} q^k$. Sorting the sequence p_c^k in increasing order, one can obtain new sequence $p_c^{(k)}$. Then, for each interval of the bottomhole pressure $(p_c^{(k)}, p_c^{(k+1)}), k = \overline{1,N}, p^{(N+1)} = p_R$ system (8) is reduced to a quadratic equation with respect to p_{bh}. One of the roots of this equation always exceeds reservoir pressure and has no physical meaning. Another root in the dimensionless form is given by

$$p_{bh}^k = 1 + \frac{1}{2C\Pi k^2} - \sqrt{\frac{1}{4(C\Pi k^2)^2} + \frac{1}{C\Pi k^2}(1 - p_{bh0})}, \quad k = \overline{1,N}. \tag{9}$$

Here reservoir pressure p_R and rate of N working fractures at minimum possible bottomhole pressure $NJ_0(p_R - p_{bh0})$ are chosen as pressure and flow rate scales, $\Pi = J_0^2 p_R/(2C_d^2\rho A^2)$.

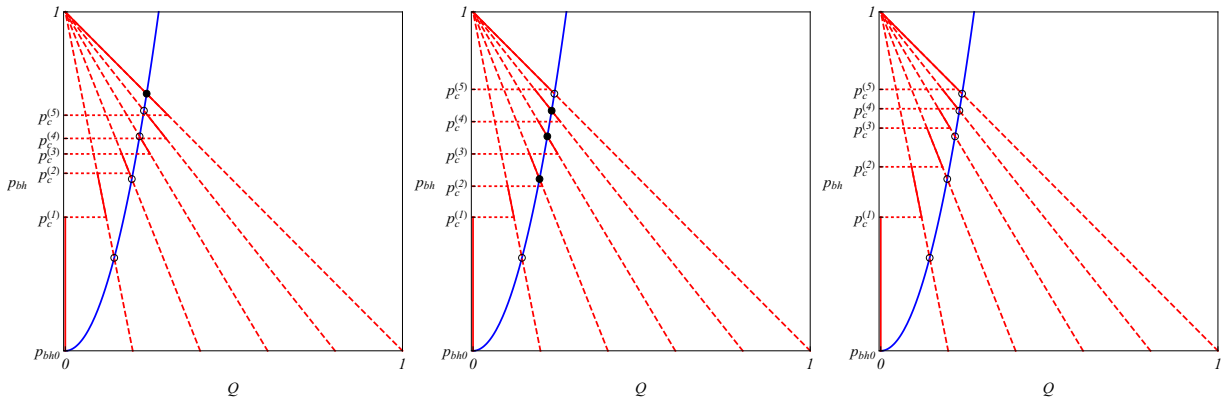

FIG. 2. Examples.

The *candidate* root p_{bh}^k must lie in the corresponding interval $(p_c^{(k)}, p_c^{(k+1)})$ to describe actual steady state of the well. Accordingly, we will say that for the given choke opening, the well has steady state if there exists at least one $k^* = \overline{1, N}$ such that $p_{bh}^{k^*} \in (p_c^{(k^*)}, p_c^{(k^*+1)})$. Otherwise, it is said that the well has no steady states.

We also suppose that during startup of the well the choke opening increases and the bottomhole pressure decreases. In this case, the system reaches the steady state with the maximum value of pressure first and stays there until further adjustment of choke opening. Consequently, we study only the steady state with the maximum value of pressure and correspondingly the maximum number of producing fractures k^*.

Figure 2 shows graphical representations of the system (8) for $N = 5$ and three different sets of $p_c^{(k)}$. Choke size is the same for all plots. The solid blue line shows the dependency of rate on the bottomhole pressure representing wellbore and choke. The solid red line shows the dependency of the total flow rate from fractures on the bottomhole pressure. Circles and disks depict candidate solutions with p_{bh}^k outside and inside corresponding intervals $(p_c^{(k)}, p_c^{(k+1)})$. The actual steady-state solution is the disk with the highest pressure. Depending on the distribution of critical pressures within the same interval, we can observe substantially different situations (from maximum number of fractures producing at the left plot to entire well collapse at the right plot) for the constant choke size. Therefore, instead of studying particular configurations of critical rates and pressures, we suggest treating them as random variables.

Now consider the critical pressures p_c^k to be identical random variables with the probability density function f and the cumulative distribution function F. The sequence of re-ordered

TABLE I. Physical parameters.

Parameter	Symbol	Unit	Case 1	Case 2	Case 3	Case 4
Reservoir pressure	p_R	psi	7000.0			7106.9
Fluid density	ρ	kg/m^3	1000.0			1000.0
Wellbore diameter	d	m	0.1			4.7
Discharge coefficient	C_d	–	0.85			0.85
True vertical depth	h	m	3000.0			3000.0
Wellhead downstream choke pressure	p_{whdc}	psi	435.0			1450.4
Fracture productivity index	J_0	bbl/day/psi	$2.5 \cdot 10^{-2}$			$6.7 \cdot 10^{-2}$
Critical volumetric flow rate	$\hat{q}_c = q_c/\rho$	bbl/day	$20.0 \div 30.0$	$10.0 \div 30.0$	$10.0 \div 20.0$	$3.3 \div 87.0$
Number of fractures	N	–	100			100

TABLE II. Dimensionless parameters.

Parameter	Symbol	Case 1	Case 2	Case 3
Minimum bottomhole pressure	p_{bh0}	0.68		
Conductivity number	Π	$2.26 \cdot 10^{-8}$		
Minimum critical pressure	p_-	0.83	0.83	0.89
Maximum critical pressure	p_+	0.89	0.94	0.94

critical pressures $p_c^{(k)}$ becomes the sequence of order statistics of the statistical sample p_c^k. Realization of k-th steady state with k fractures working is now a random event. Below we will calculate the probability P_k associated with it.

The joint probability distribution function of order statistics $p_c^{(k)}, \ldots, p_c^{(N)}$ is calculated as follows [1]

$$f_k(p_c^{(k)}, \ldots, p_c^{(N)}) = \frac{N!}{(k-1)!} F(p_c^{(k)})^{k-1} \prod_{i=k}^{N} f(p_c^{(i)}) \theta(p_c^{(i+1)} - p_c^{(i)}). \tag{10}$$

Let $\mathcal{A}(k, C)$ be the event describing that k fractures are producing at choke opening C.

The probability of $\mathcal{A}(k,C)$ (i.e., the k-th steady state is reached) is given by

$$P_k = P(\mathcal{A}(k,C)) = \underbrace{\int\cdots\int}_{N-k+1} \prod_{i=k}^{N} dp_c^{(i)} \times f_k(p_c^{(k)},\ldots,p_c^{(N)}) \times \theta(p_{bh}^k - p_c^{(k)})\theta(p_c^{(k+1)} - p_{bh}^k)\times$$
$$\times \prod_{i=k+1}^{N} [\theta(p_c^{(i)} - p_{bh}^i) + \theta(p_{bh}^i - p_c^{(i+1)})]. \tag{11}$$

Here the integration is carried out over any suitable interval containing the support of f. The product of the first two theta-functions shows that the k-th candidate pressure (9) is between the k-th and $k+1$-th critical pressures. The rest factors show that all candidate pressures larger than k-th lie outside of corresponding intervals. Calculation of P_k is outlined in Appendix A.

For illustration purposes, we consider only the case of the uniform distribution f. The probability density function $f(x)$ and cumulative distribution $F(x)$ in this case are given by

$$f(x) = \frac{1}{p_+ - p_-}\theta(x - p_-)\theta(p_+ - x), \tag{12}$$

$$F(x) = \frac{x - p_-}{p_+ - p_-}\theta(x - p_-)\theta(p_+ - x) + \theta(x - p_+). \tag{13}$$

However, the procedure presented in Appendix A is valid for an arbitrary probability distribution.

Note that the integral in Eq. (11) depends only on the values of candidate pressures p_{bh}^k. This means that the probability calculations and physical model are well separated. Therefore, it is possible to use a more sophisticated description of wellbore flow as compared to Eq. (3) and/or inflow performance relationship different from Eq. (7) to produce the sequence of p_{bh}^k.

The bottomhole pressure, total flow rate, and number of surviving fractures are now random variables with some probability distributions. In the next section, we will qualitatively analyze these distributions.

IV. QUALITATIVE ANALYSIS

We expect the following schematic picture of different probability distributions under varying choke size. If the maximum candidate pressure p_{bh}^N is above the value p_+ the well

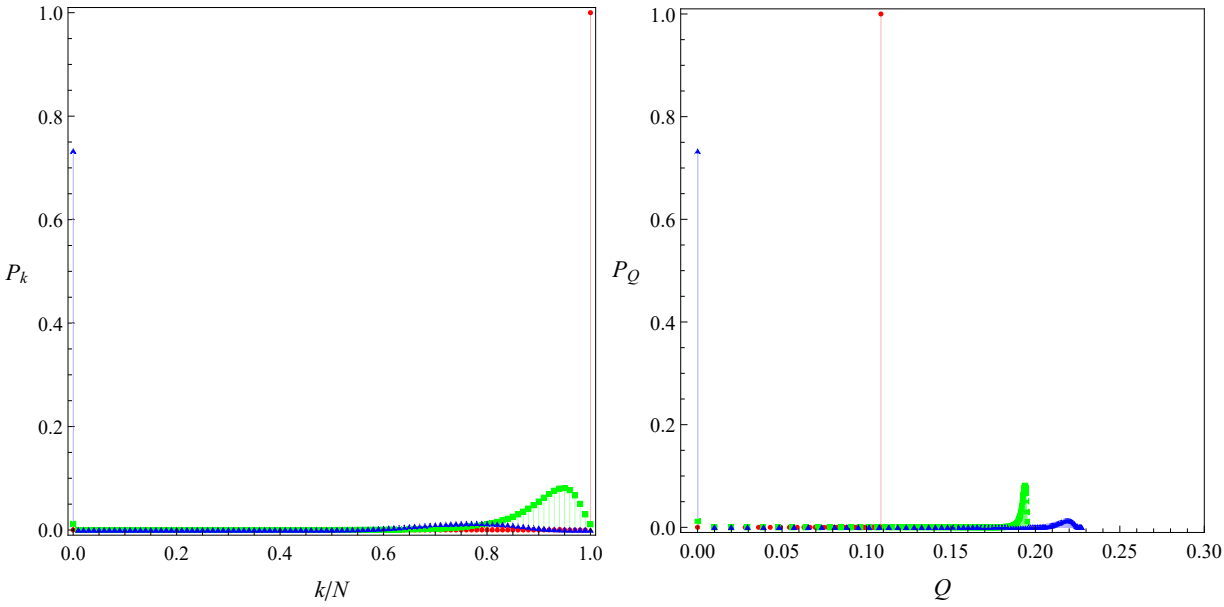

FIG. 3. Probability distributions for the number of producing fractures and the total rate.

is operated under safe conditions and all N fractures are producing, $P_N = 1$. These conditions are met for sufficiently small choke openings. After choke size exceeds certain value corresponding to the condition $p_{bh}^N = p_+$ all steady states with $k = \overline{0, N}$ fractures producing are possible. Probability of the entire system collapse P_0 grows with increase of choke size and becomes equal to unity at the opening defined by $p_{bh}^N = p_-$.

Figure 3 illustrates the evolution of probability distributions of the number of producing fractures and the total flow rate for the parameters summarized in Table I, case 1, and the choke sizes $8/64''$ (red), $11/64''$ (green), $12/64''$ (blue). For the smallest choke size, the well is in the safe zone (all fractures produce) but the drawdown and the rate are low. For the intermediate choke opening, the drawdown is higher but the probability of failure of several fractures is non-zero. For the largest choke size, all fractures lose conductivity with very high probability, however, if some of them are not damaged, the well total production is relatively high.

Another way to analyze the behavior of the well is the analysis of the moments of the number of producing fractures k and the total flow rate Q. For such analysis, introduce the

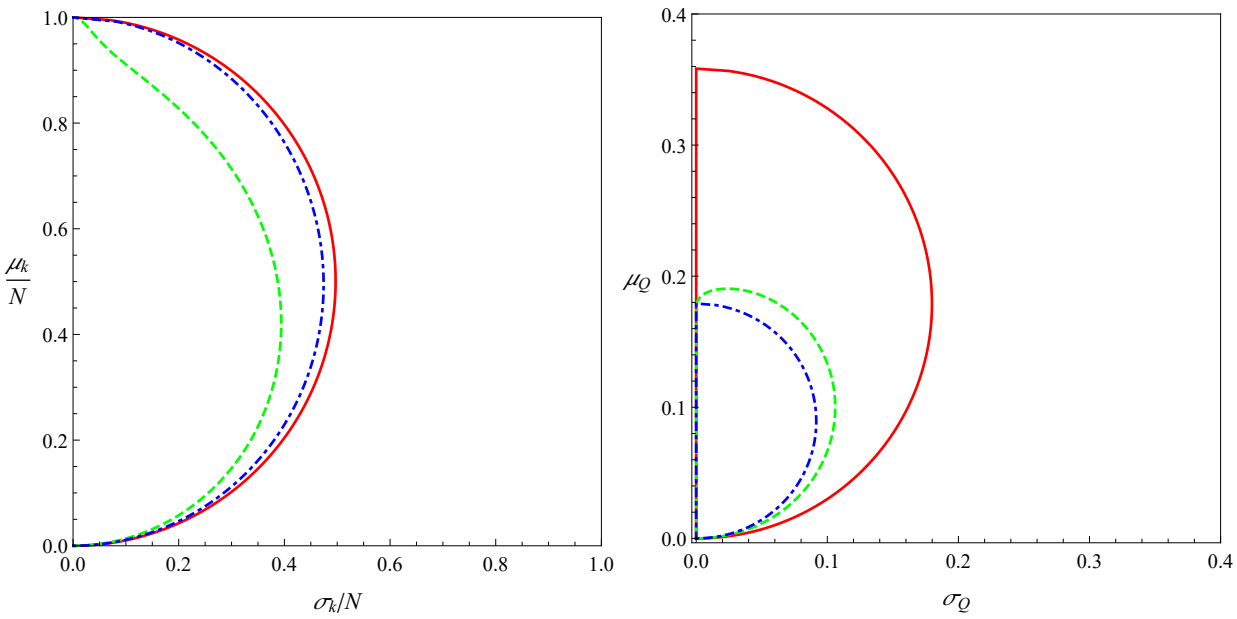

FIG. 4. Parametric plots mean value vs. dispersion.

expected values and variances

$$\mu_k = \sum_{k=1}^{N} P_k k, \quad \sigma_k^2 = \sum_{k=1}^{N} P_k k^2 - \mu_k^2,$$
$$\mu_Q = \sum_{k=1}^{N} P_k Q_k, \quad \sigma_Q^2 = \sum_{k=1}^{N} P_k Q_k^2 - \mu_Q^2.$$

Here the rate Q_k corresponds to k producing fractures and is given by

$$Q_k = \frac{1 - p_{bh}^k}{1 - p_{bh0}} \frac{k}{N}.$$

Figure 4 shows plots of the parametric curves $(\sigma_k(d_{ch}), \mu_k(d_{ch}))$ and $(\sigma_Q(d_{ch}), \mu_Q(d_{ch}))$ for the parameters given in Table I, cases 1 (red), 2 (green), and 3 (blue). Expectation of the number of producing fractures monotonically decreases with increase of the choke size. If our goal is to protect the maximum number of fractures, the only strategy is to keep the bottomhole pressure far from the dangerous range. If our goal is the high flow rate or both high rate and number of producing fractures, the right strategy of managing the choke opening is not so obvious. If we are concerned with the rate only, the natural desire is to get the maximum rate (characterized by the expected value μ_Q) at the minimum uncertainty (characterized by the variance σ_Q). As one can see from Figure 4, it is not possible to reach both extrema simultaneously. A possible solution may be to specify some acceptable level of

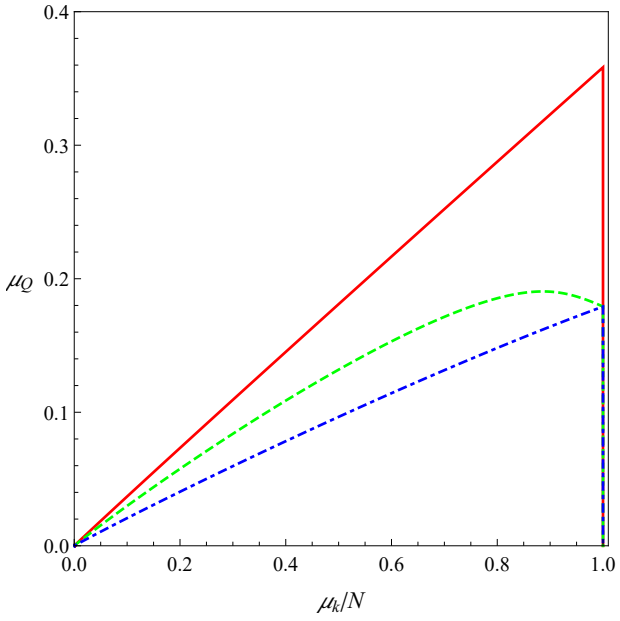

FIG. 5. Parametric plot of the mean number of producing fractures vs. mean rate.

absolute or normalized variance that we could tolerate and optimize the μ_Q under constrain of σ_Q bounded by this tolerance.

Another observation can be made using Figure 5 (color coding and parameters as in Figure 4). From this figure, it is clearly seen that the maximum flow rate might correspond to the number of producing fractures significantly lower than N (case 2, green). One can interpret this fact in the following way. It is possible to choose aggressive choke management strategy systematically and damage recently created fractures without obvious manifestation of this damage in the surface flow rate.

V. CORRECTION OF EXPECTATIONS BASED ON OBSERVATIONS & CHOKE MANAGEMENT POLICY

In Section III we formulated some expectations about the state of the well for a given choke size in terms of associated probabilities. These expectations do not take into account information that may be acquired during the actual process of well startup. Consider the well that already passed through the set of M states characterized by the value of choke size d_{ch}^m or the values of C_m, $m = \overline{1, M}$. Using the recorded values of the total flow rate at the previous choke sizes and the value of an individual fracture conductivity J_0 (supposed to

be known), one can obtain the numbers k_m of surviving fractures corresponding to the C_m. Below we will try to use this information about the past performance of the well to correct our expectations about its future behavior.

The probability of the event that $k = k_0$ fractures will produce at choke opening $C = C_0$ given that k_1 fractures produced at choke opening C_1, k_2 at C_2, ..., k_M at C_M is the conditional probability given by

$$P_{(k_0,C_0)|(k_1,C_1),\ldots,(k_M,C_M)} = P\left(\mathcal{A}(k_0,C_0)\middle|\bigcap_{m=1}^{M}\mathcal{A}(k_m,C_m)\right) = \frac{P\left(\bigcap_{m=0}^{M}\mathcal{A}(k_m,C_m)\right)}{P\left(\bigcap_{m=1}^{M}\mathcal{A}(k_m,C_m)\right)}. \quad (14)$$

Both numerator and denominator of the fraction in (14) are defined similarly as in Eq. (11):

$$P\left(\bigcap_{m=m_0}^{M}\mathcal{A}(k_m,C_m)\right) = \underbrace{\int\cdots\int}_{N-k_{m_0}+1}\prod_{i=k_{m_0}}^{N} dp_c^{(i)} \times f_{k_{m_0}}(p_c^{(k_{m_0})},\ldots,p_c^{(N)})\times$$

$$\times\prod_{m=m_0}^{M}\left[\theta(p_{bh}^{k_m}(C_m)-p_c^{(k_m)})\theta(p_c^{(k_m+1)}-p_{bh}^{k_m}(C_m))\prod_{i=k_m+1}^{N}[\theta(p_c^{(i)}-p_{bh}^{i}(C_m))+\theta(p_{bh}^{i}(C_m)-p_c^{(i+1)})]\right]. \quad (15)$$

Here $m_0 = 0$ for the numerator and $m_0 = 1$ for the denominator in (14). Each factor in the outer product is similar to the product of theta-functions in (11). Note that here we should distinguish the candidate bottomhole pressure corresponding to the different choke sizes. From the assumption that the choke size increases in time, it follows that $C_{m+1} < C_m$ and $p_{bh}^{i}(C_{m+1}) < p_{bh}^{i}(C_m)$, $\forall i, m$. Because the fractures lose productivity irreversibly, the number of surviving fractures in future is always smaller or equal to the number of fractures surviving in the past so that $k_m \leq k_{m+1}$, $\forall m$.

Calculation of $P_{(k_0,C_0)|(k_1,C_1),\ldots,(k_M,C_M)}$ is outlined in Appendix B. A noteworthy result of this calculation is that under assumptions given above, $P_{(k_0,C_0)|(k_1,C_1),\ldots,(k_M,C_M)} = P_{(k_0,C_0)|(k_1,C_1)}$. This means that all probability distributions are affected only by the last observed state of the well. In other words, it does not matter how exactly (in what particular order and by what sequence of choke sizes) fractures have been damaged. Only the most recent observation helps to correct our future expectations about the well behavior.

The independence of the conditional probability on the previous states, except the last one, means that the process of well evolution is Markovian. This allows us to apply to the

problem of proper choke management strategy a formalism of Markov decision processes (MDP) [8, 11].

We will refer to the pair (*number of intact fractures, current choke parameter*) as the state of well $s = (k, C)$. In the subsequent derivations, we consider the choke parameter C to be from the finite set $\mathbb{C}_L = \{C_l\}_{l=1}^{L}$, for example induced by uniform step of choke size adjustment. This assumptions significantly simplifies problem statement. Let us denote the set of all possible states $\mathbb{S} = \mathbb{Z}_{N+1} \times \mathbb{C}_L$ and the set of available at the state s actions a (choke parameters adjustments) $\mathbb{A}_s = \{a \in \mathbb{C} : a \leq C\}$. Probabilities $P_{ss'}^a$ of transition from state $s = (k, C)$ to state $s' = (k', C')$ under action a have been calculated in the previous section $P_{ss'}^a = P_{(k',C')|(k,C)}$. Note that $P_{ss'}^a = 0, \forall k' > k, \forall C' \neq a, \forall a > C$. Finally, let us define an immediate reward function of the transition $s \to s'$ under action a as a difference between total flow rate at the states s' and s, $r_{ss'}^a = Q_{k'}(a = C') - Q_k(C)$. The problem of MDP is to find a policy $\Pi : \mathbb{S} \to \mathbb{A}_s$ maximizing expected value of sum of the random immediate rewards

$$V = \sum_{t=1}^{L} r_{s_t s_{t+1}}^{a_t}.$$

Here actions are chosen according to policy, e.g., $a_t = \Pi(s_t)$. The horizon of planning is finite and equal to L because we assume that the set of possible choke sizes is finite and choke opening can only increase in time. The problem considered is equivalent to maximization of the final total flow rate, one of the possible goals discussed in the Section IV.

We apply the well known value iteration algorithm [3] to the MDP problem described above. After the policy is found, evaluation of the number of producing fractures is required to determine the current state s_t and define the next action a_t. Throughout the paper, we use the assumption that the productivity index of the individual fractures are equal. Accordingly, the number of producing fractures may be calculated using the measured flow rate. This assumption is essential for application of MDP to our problem because it reflects fundamental assumption of MDP formalism that the environment is fully observable and the current state completely characterizes the process.

Figure 6 graphically illustrates the optimal policy calculated for the parameters listed in Table I, Case 4, and the range of choke parameters $\mathbb{C}_L$ corresponding to openings $8/64'', 12/64'', ..., 52/64''$. Each point of the diagram corresponds to state s, current choke opening is the horizontal coordinate and observed number of producing fractures relative

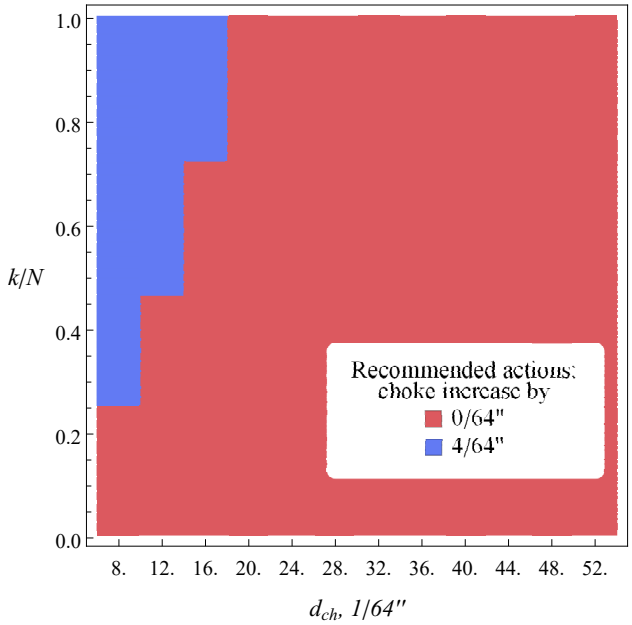

FIG. 6. Choke management policy.

to total number of fractures is the vertical coordinate. Color shows the optimal action for the state, either increase choke opening for some value or keep it constant. As one can note, for the majority of states, the optimal policy recommends keeping choke opening constant. In particular, for the choke sizes larger than $20/64''$, there are no observed number of producing fractures such that any action will increase the expected value of the final flow rate. However, for the lower openings and relatively high number of surviving fractures, it is reasonable to increase the choke further. Note that the increase of the choke by more than one step at once is never optimal. This conclusion seems to be natural and may be interpreted as follows. Choke adjustments not only increase flow rate but also allow gaining information about statistics of critical rates. Cautious choke opening in small steps helps collect the information gradually without additional risk of damaging fractures and utilize it at the next steps.

VI. NUMERICAL AND ANALYTICAL SIMULATIONS

For additional illustration of cascading failure in the system of interacting hydraulic fractures and to compare predictions of statistical and deterministic approach, we performed numerical and analytical modeling of the fracture-wellbore system as shown in Fig.1 The

models simulated single-phase incompressible flow in the horizontal well connected with 100 hydraulic fractures with parameters similar to Case 4 in Table I. The simulated well has a 3000 m long vertical section and a 2000 m long horizontal section. The fractures are placed equidistantly along the horizontal section and have identical spatial dimensions (20 m height, 100 m half-length). All fractures are assumed to have constant 5 mm width and to be uniformly propped with permeability of the proppant pack equal to 1440 darcy. Rates of inflows from the reservoir into each cell element of the fractures are proportional to the difference between the fluid pressure in the cell and far field pore pressure. Selected fracture conductivity is high enough to neglect pressure variation along the fracture. As a result, all fractures effectively have the same constant productivity index J_0. The initial reservoir pressure is 490 bar. The wellhead pressure downstream choke (WHDCP) was fixed at 100 bar. The pressure drop and associated fluid production are controlled by gradual opening of the wellhead choke from 3/64" to 28/64". We were prescribing different critical velocity or, equivalently, different critical flow rate for each fracture in the range from 0.25 m^3/d to 6.9 m^3/d.

In the numerical model, we coupled the model of the transient flows in a well, described in [14], with the numerical models of individual fractures. Each fracture was represented by a grid of conductive cells with fixed width simulating a porous medium. Single-phase incompressible flow in these porous cells was described by a standard Darcy's equation [17] with constant viscosity and permeability of the proppant pack. If the flow rate from the fracture exceeded the critical value, all cells connecting the fracture to the well were updated with zero conductivity. The well and fracture models were coupled using iterative algorithm based on Picard iterations (or fixed point iterations method) [9] that ensured balance of pressures and flow rates between them within certain tolerance.

In the analytical model, we performed fine timestepping such that there could be more time steps between choke changes than total number of fractures and all fractures could potentially lose their productivity in the cascading failure sequence after a single choke increase. At a given timestep, the model would either increase the choke if it is prescribed by the choke schedule or reduce the number of producing fractures based on the comparison of the current flow rate and critical ones. Every time step also updates flow rates and bottomhole pressure. This ensures that immediate increase of production caused by the choke increase is recorded before some of the fractures are failed and there is a non-zero

response time of fracture conductivity to the choke change. The analytical model neglects viscous pressure losses along the well, which in case of incompressible fluid allows defining updates of flow rates and bottomhole pressure as explicit functions of choke size and number of fractures.

Fig. 7 represents the comparison of the numerical and analytical models for the specific choice of critical fracture flow rates. In fig. 7 the critical flow rates monotonically and uniformly increase from the lowest (0.25 m^3/d) to the highest (6.9 m^3/d). The wellhead choke is gradually opened from 3/64" to 28/64" during the first 25 hours, making a stepwise increase of 1/64" every hour. Note that the choice of the uniform distribution of critical velocities in deterministic approach is made because a) it has the same mean as uniform random distribution and b) it resembles the uniform probability density function used in the statistical description above. However, it is not guaranteed that evolution with time or with choke size of this specific realization of the ensemble of critical fracture velocities would be equivalent to evolution of expected values of variables predicted by statistical approach.

Fig. 7 illustrates the dynamics of choke size change, bottomhole pressure, production rate, and number of surviving producing fractures during the first 25 hours of flowback. Each step of choke opening is associated with a stepwise decrease of bottomhole pressure and stepwise increase of production rate. This corresponds to vertical segments on the charts representing pressures and flow rates as functions of time and number of fractures. More specifically, on the chart of total production rate as function of the number of production fractures, each timestep is denoted by a marker. After the production rate rises vertically due to a stepwise choke increase, the curve goes left and downward due to the failure of individual fractures. The reduced number of producing fractures redistributes the flow rates, which can cause further reduction in the number of producing fractures at the next timesteps and this cascade of fracture failures continues until the stable number of fractures is found or all fractures lose conductivity. In this case, the total production rate reaches its peak at about 50 producing fractures. Soon after that, there is the last stable combination of the choke size, rate, and number of fractures. The next increase of the choke size leads to the fast failure of the rest of the producing fractures in the final cascading event until all fractures in the well are completely closed and production is terminated. Results of the numerical simulation are in good agreement with the analytical model predictions.

Fig. 8 compares the total production rate versus number of producing fractures obtained

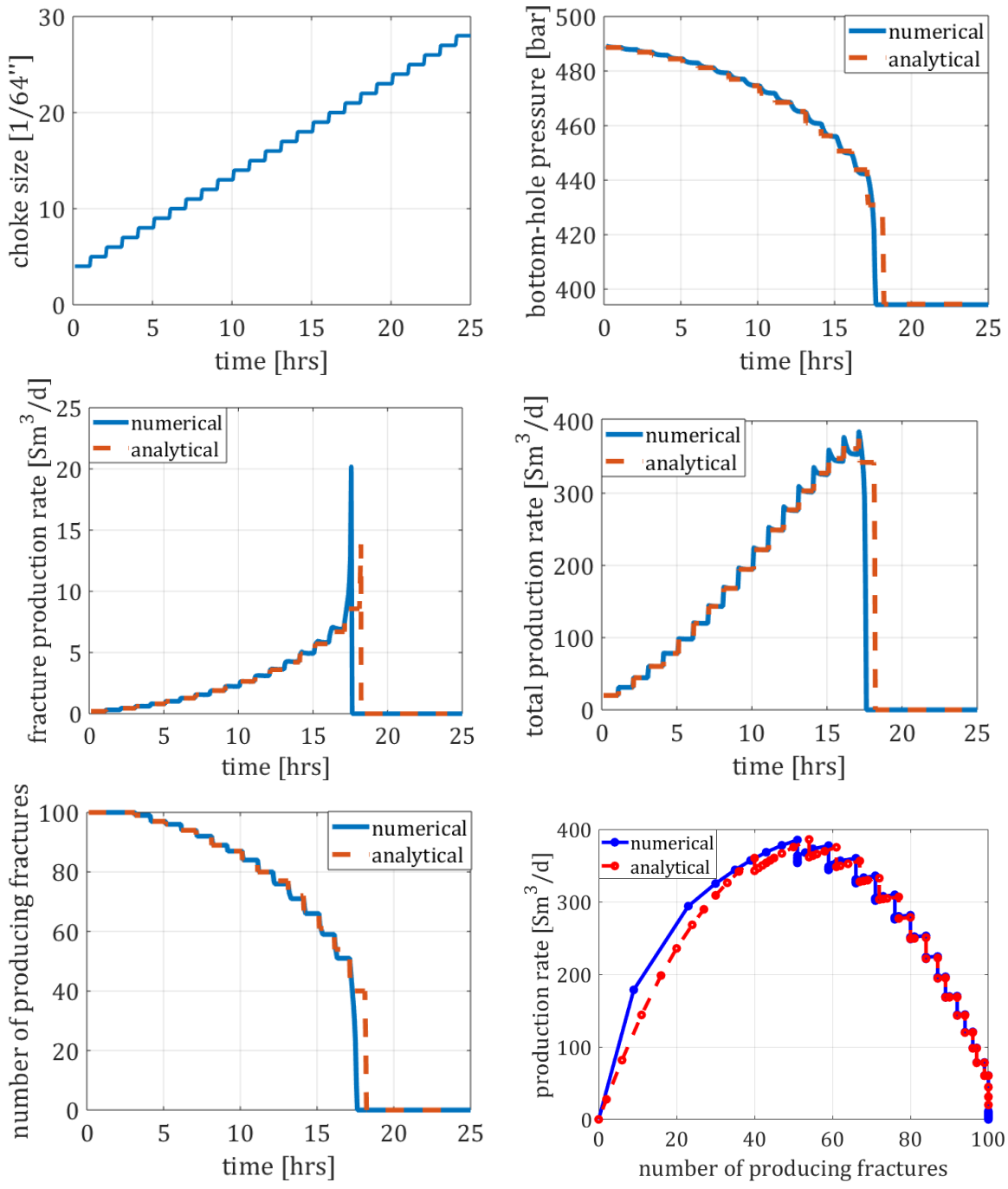

FIG. 7. Numerical simulation results.

with numerical model, analytical model, statistical description and Monte-Carlo simulations. Monte-Carlo (MC) simulations were built bu running the analytical model $4 * 10^6$ times (4M) with uniform random distribution of critical fracture rates in the same range as in the statistical model. In the MC simulations, the choke was gradually opened in the same range

from 3/64" to 28/64" with the finer step of 1/6400". Then, for each combination of the choke setting and observed number of producing fractures, we accumulated number of trajectories crossing that point. For each given choke opening we accumulate density distribution of observed number of producing fractures. It is straightforward to calculate average number of producing fractures from this distribution. As shown in fig. 8, the mean number of producing fractures as function of choke opening follows the same path in MC simulations, in statistical approach and also in the numerical and analytical model with uniform distribution of critical rates. This indicates, that it is possible to reproduce "mean" behavior of the fracture system by a single deterministic numerical simulation with correctly chosen distribution of critical rates. This can be useful, if it is necessary to analyze details of the processes occurring inside the fractures during cascading failure process, under conditions, that are identified as "typical" or somehow important by the statistical analysis.

Using the density distribution of the number of producing fractures as function of choke opening it is also straightforward to calculate average production rate corresponding to the mean number of producing fractures. Since all in the model fractures have the same productivity index, for the fixed choke opening each number of fractures in the distribution can be easily recalculated into a certain total production rate. After the convolution of this rate with distribution density one can calculate average rate as function of choke opening for all realizations. Fig. 8 essentially plots the average flow rate versus average number of producing fractures parameterized by the same value of choke opening.

Comparison of numerical, analytical, statistical and Monte-Carlo calculations represented in fig. 8 shows that there is good agreement between all of them. We would argue that all of them can be used interchangeably as needed and as allowed by the requirements of the problem that needs to be analyzed. This can be useful for engineering purposes, when, for example, it is necessary to analyze details of the mechanism of fracture conductivity damage inside fractures for some specific realization of fracture properties. The statistical or Monte-Carlo approach can be used first to identify the specific scenario or the trajectory in the total rate versus choke opening space. Then, analytical model can be used to convert rate versus choke curve into the specific realization of critical rates distribution. The latter can be simulated with the numerical model to analyze details of the fracture damage mechanisms and investigate options to re-engineer fracture properties.

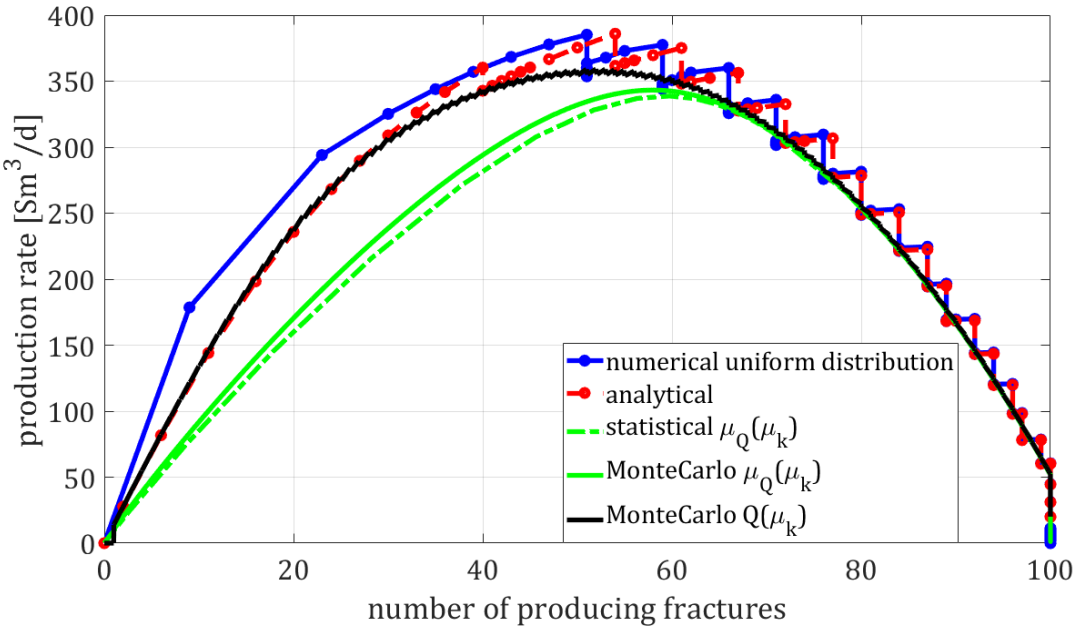

FIG. 8. Numerical simulation results.

VII. CONCLUSION

In this work, the emergent behaviour leading to the formation of the cascading failure mechanism in multistage hydraulically fractured wells during well startup and initial production is described and investigated. This phenomenon can be explained by existence of a feedback loop due to the hydraulic connection between individual producing fractures connected to the same wellbore. In our study, we presented several possible scenarios of evolution of cascading failure. The failure of weaker hydraulic fractures in such systems might increase drawdown on the stronger fractures, which survive. In turn, some of surviving fractures are weaker than others, so further increase of drawdown might lead to the cascading failure of an ever-increasing amount of fractures. We also evaluated specific conditions triggering the cascading failure effect. To the best of our knowledge, the phenomenon of cascading failure of hydraulic fractures has not been studied in the previously published literature.

The hydraulic fracturing process is associated with a lack of robust measurement techniques and hence it is intrinsically uncertain. This provides grounds for treating the hydraulically fractured systems using a probabilistic approach and assuming that the failure criterion is represented as a random variable. Based on the proposed description, the analy-

sis of the full system behavior is carried out. As an outcome, several choke opening strategies during the well startup could are formulated. Overall, these strategies deal with the trade-off between the short-term goal of maximizing production and long-term goal of preserving a larger number of hydraulic fractures. It is shown that moderate choke openings favor the well operating in the safe zone with productivity of all fractures preserved at the cost of relatively low production rates. Intermediate values of choke opening might lead to damage of some fractures; however, the production rates will be higher. Finally, the aggressive and large choke opening in extreme cases can lead to damage of all fractures. However, if some fractures survive with this strategy, a high production rate could be achieved. For the particular strategy aiming to maximize production rate, we propose a way to calculate choke management policy taking into account the statistical nature of fractures properties. Given the current number of producing fractures and choke opening, the policy defines the next choke adjustment maximizing the expected value of the final flow rate.

Finally, the evolution of cascading failure is demonstrated using numerical simulations that are based on fewer assumptions than analytical model and probabilistic description. It is shown that numerical results coincide qualitatively and quantitatively with the probabilistic description for the system with large number of hydraulic fractures.

ACKNOWLEDGEMENTS

The authors are grateful to Schlumberger for permission to publish this work.

Appendix A: Calculation of prior probabilities

First, let us make the following change of variables in (11):

$$\omega_k = F(p_c^{(k)}), \quad \pi_k = F(p_{bh}^k). \tag{A1}$$

Next, the product of theta-functions in (11) may be transformed to

$$\begin{aligned}
&\theta(p_{bh}^k - p_c^{(k)})\theta(p_c^{(k+1)} - p_{bh}^k) \prod_{i=k+1}^{N} [\theta(p_c^{(i)} - p_{bh}^i) + \theta(p_{bh}^i - p_c^{(i+1)})] = \\
&= \theta(\pi_k - \omega_k)\theta(\omega_{k+1} - \pi_k) \prod_{i=k+1}^{N} [\theta(\omega_i - \pi_i) + \theta(\pi_i - \omega_{i+1})] = \\
&= \theta(\pi_k - \omega_k)\theta(\omega_{k+1} - \pi_k) \prod_{i=k+1}^{N-2} [\theta(\omega_i - \pi_i) + \theta(\pi_i - \omega_{i+1})] \times \\
&\qquad \times [\theta(\omega_{N-1} - \pi_{N-1}) + \theta(\pi_{N-1} - \omega_N)]\theta(\omega_N - \pi_N) = \\
&= \theta(\pi_k - \omega_k)\theta(\omega_{k+1} - \pi_k) \prod_{i=k+1}^{N-2} [\theta(\omega_i - \pi_i) + \theta(\pi_i - \omega_{i+1})] \times \\
&\qquad \times \theta(\omega_{N-1} - \pi_{N-1})\theta(\omega_N - \pi_N) = \cdots = \\
&= \theta(\pi_k - \omega_k) \prod_{i=k+1}^{N} \theta(\omega_i - \pi_i)
\end{aligned} \tag{A2}$$

The latter transformation takes into account that $\pi_{k+1} > \pi_k$ and consequently

$$\theta(\pi_{k-1} - \omega_k)\theta(\omega_k - \pi_k) \equiv 0.$$

Then, using (10) one can obtain

$$\begin{aligned}
P_k &= \underbrace{\int_0^1 \cdots \int_0^1}_{N-k+1} \prod_{i=k}^{N} d\omega_i \, \theta(\omega_{i+1} - \omega_i)\theta(\pi_k - \omega_k) \prod_{i=k+1}^{N} \theta(\omega_i - \pi_i) \frac{N!}{(k-1)!} \omega_k^{k-1} = \\
&= \int_0^1 d\omega_N \theta(\omega_N - \pi_N) \underbrace{\int_0^1 \cdots \int_0^1}_{N-k} \prod_{i=k}^{N-1} d\omega_i \, \theta(\omega_{i+1} - \omega_i)\theta(\pi_k - \omega_k) \prod_{i=k+1}^{N-1} \theta(\omega_i - \pi_i) \frac{N!}{(k-1)!} \omega_k^{k-1}.
\end{aligned} \tag{A3}$$

Rearranging integration order one can get

$$
\begin{aligned}
P_k = \frac{N!}{(k-1)!}\int_0^1 d\omega_N \int_0^1 d\omega_{N-1}\theta(\omega_N-\pi_N)\theta(\omega_N-\omega_{N-1})\times\cdots\times \\
\times\int_0^1 d\omega_{k+1}\theta(\omega_{k+2}-\pi_{k+2})\theta(\omega_{k+2}-\omega_{k+1})\times \\
\times\int_0^1 d\omega_k\omega_k^{k-1}\theta(\omega_{k+1}-\pi_{k+1})\theta(\omega_{k+1}-\omega_k)\theta(\pi_k-\omega_k) = \\
= \frac{N!}{k!}\pi_k^k\int_0^1 d\omega_N\theta(\omega_N-\pi_N)\int_0^1 d\omega_{N-1}\theta(\omega_{N-1}-\pi_{N-1})\theta(\omega_N-\omega_{N-1})\times\cdots\times \\
\times\int_0^1 d\omega_{k+2}\theta(\omega_{k+3}-\omega_{k+2})\theta(\omega_{k+2}-\pi_{k+2})\times \\
\times\int_0^1 d\omega_{k+1}\theta(\omega_{k+2}-\omega_{k+1})\theta(\omega_{k+1}-\pi_{k+1}) = \\
= \frac{N!}{k!}\pi_k^k\int_0^1 d\omega_N\theta(\omega_N-\pi_N)\int_0^1 d\omega_{N-1}\theta(\omega_{N-1}-\pi_{N-1})\theta(\omega_N-\omega_{N-1})\times\cdots\times \\
\times\int_0^1 d\omega_{k+2}\theta(\omega_{k+3}-\omega_{k+2})\theta(\omega_{k+2}-\pi_{k+2})\theta(\omega_{k+2}-\pi_{k+1})(\omega_{k+2}-\pi_{k+1}).
\end{aligned}
$$

The latter transformation takes again into account that $\pi_{k+1} > \pi_k$ and

$$\theta(\omega_{k+1}-\pi_{k+1})\theta(\omega_{k+1}-\pi_k) \equiv \theta(\omega_{k+1}-\pi_{k+1}).$$

Let us define a sequence of functions

$$g_{k,l+1}(\omega_{l+1}) = \int_0^1 d\omega_l\theta(\omega_{l+1}-\omega_l)\theta(\omega_l-\pi_l)g_{k,l}(\omega_l). \tag{A4}$$

Here index $l = \overline{k+2, N+1}$ and the starting member of the sequence is

$$g_{k,k+2}(\omega_{k+2}) = \theta(\omega_{k+2}-\pi_{k+1})(\omega_{k+2}-\pi_{k+1}). \tag{A5}$$

Using the previous definition, one can rewrite the equation for probability as

$$P_k = \frac{N!}{k!}\pi_k^k\int_0^1 d\omega_N\theta(\omega_N-\pi_N)g_{k,N}(\omega_N) = \frac{N!}{k!}\pi_k^k\theta(1-\pi_N)g_{k,N+1}(1). \tag{A6}$$

One can check by the direct substitution into (A4) that the functions $g_{k,l}(\omega_l)$ are polynomials multiplied by appropriate theta function:

$$g_{k,l}(\omega_l) = \theta(\omega_l-\pi_{l-1})\sum_{i=0}^{l-k-1} a_{k,l,i}\omega_l^i, \quad l = \overline{k+2, N+1}. \tag{A7}$$

Coefficients of polynomials for successive indexes l are related in the following way:

$$a_{k,l+1,i+1} = \frac{a_{k,l,i}}{i+1}, \quad i = \overline{0, l-k-1}, \quad a_{k,l+1,0} = -\sum_{i=0}^{l-k-1}\frac{a_{k,l,i}}{i+1}\pi_l^{i+1}. \tag{A8}$$

Equations (A8) and (A5) allow recursive calculation of polynomial coefficients for $g_{k,N+1}$ and, thus, probability P_k according to (A6).

Appendix B: Calculation of conditional probabilities

First, let us use again the change of variables (A1) and the result (A2) to transform the product of theta-functions in (15)

$$\prod_{m=m_0}^{M}\theta(p_{bh}^{k_m}(C_m)-p_c^{(k_m)})\theta(p_c^{(k_m+1)}-p_{bh}^{k_m}(C_m))\prod_{i=k_m+1}^{N}[\theta(p_c^{(i)}-p_{bh}^{i}(C_m))+\theta(p_{bh}^{i}(C_m)-p_c^{(i+1)})]=$$
$$=\prod_{m=m_0}^{M}\theta(\pi_{k_m}(C_m)-\omega_{k_m})\prod_{i=k_m+1}^{N}\theta(\omega_i-\pi_i(C_m))$$

Next, using the conditions $\pi_i(C_{m+1}) < \pi_i(C_m)$, $\forall i,m$ and $k_m \le k_{m+1}$, $\forall m$, one can transform the latter equation:

$$\prod_{m=m_0}^{M}\theta(\pi_{k_m}(C_m)-\omega_{k_m})\prod_{i=k_m+1}^{N}\theta(\omega_i-\pi_i(C_m))=$$
$$=\prod_{m=m_0}^{M}\theta(\pi_{k_m}(C_m)-\omega_{k_m})\left[\prod_{i=k_m+1}^{k_{m+1}-1}\theta(\omega_i-\pi_i(C_m))\right]\theta(\omega_{k_{m+1}}-\pi_{k_{m+1}}(C_m)).$$

Then, using (10) one can get

$$P\left(\bigcap_{m=m_0}^{M}\mathcal{A}(k_m,C_m)\right)=\underbrace{\int\cdots\int}_{N-k_{m_0}+1}\prod_{i=k_{m_0}}^{N}d\omega_i\,\theta(\omega_{i+1}-\omega_i)\,\frac{N!}{(k_{m_0}-1)!}\omega_{k_{m_0}}^{k_{m_0}-1}\times$$
$$\times\prod_{m=m_0}^{M}\theta(\pi_{k_m}(C_m)-\omega_{k_m})\left[\prod_{i=k_m+1}^{k_{m+1}-1}\theta(\omega_i-\pi_i(C_m))\right]\theta(\omega_{k_{m+1}}-\pi_{k_{m+1}}(C_m)).\qquad\text{(B1)}$$

Change of integration order gives

$$P\left(\bigcap_{m=m_0}^{M}\mathcal{A}(k_m,C_m)\right)=\underbrace{\int\cdots\int}_{N-k_{m_0+1}+1}\prod_{i=k_{m_0+1}}^{N}d\omega_i\,\theta(\omega_{i+1}-\omega_i)\times\theta(\omega_{k_{m_0+1}}-\pi_{k_{m_0+1}}(C_{m_0}))\times$$
$$\times\prod_{m=m_0+1}^{M}\theta(\pi_{k_m}(C_m)-\omega_{k_m})\left[\prod_{i=k_m+1}^{k_{m+1}-1}\theta(\omega_i-\pi_i(C_m))\right]\theta(\omega_{k_{m+1}}-\pi_{k_{m+1}}(C_m))\times$$
$$\times\underbrace{\int\cdots\int}_{k_{m_0+1}-k_{m_0}}\prod_{i=k_{m_0}}^{k_{m_0+1}-1}d\omega_i\,\theta(\omega_{i+1}-\omega_i)\theta(\pi_{k_{m_0}}(C_{m_0})-\omega_{k_{m_0}})\left[\prod_{i=k_{m_0}+1}^{k_{m_0+1}-1}\theta(\omega_i-\pi_i(C_{m_0}))\right]\frac{N!}{(k_{m_0}-1)!}\omega_{k_{m_0}}^{k_{m_0}-1}.$$

Comparing the last line of the previous equation with the relation for prior probability (A3) and utilizing the definition given by (A4) one can obtain

$$P\left(\bigcap_{m=m_0}^{M}\mathcal{A}(k_m,C_m)\right)=\underbrace{\int\cdots\int}_{N-k_{m_0+1}+1}\prod_{i=k_{m_0+1}}^{N}d\omega_i\,\theta(\omega_{i+1}-\omega_i)\,\frac{N!}{k_{m_0}!}\pi_{k_{m_0}}^{k_{m_0}}(C_{m_0})g_{k_{m_0},k_{m_0+1}}(\omega_{k_{m_0+1}};C_{m_0})\times$$

$$\times\prod_{m=m_0+1}^{M}\theta(\pi_{k_m}(C_m)-\omega_{k_m})\left[\prod_{i=k_m+1}^{k_{m+1}-1}\theta(\omega_i-\pi_i(C_m))\right]\theta(\omega_{k_{m+1}}-\pi_{k_{m+1}}(C_m)). \qquad \text{(B2)}$$

Here the argument C_{m_0} in the term $g_{k_{m_0},k_{m_0+1}}(\omega_{k_{m_0+1}};C_{m_0})$ shows that the values $\pi_l(C_{m_0})$ have been used to construct the polynomial $g_{k_{m_0},k_{m_0+1}}$ by formulas (A7), (A8).

Because the equations (B1) and (B2) differ only by the change of index $m_0 \to m_0+1$ and replacement of the factor

$$\frac{N!}{(k_{m_0}-1)!}\omega_{k_{m_0}}^{k_{m_0}-1}\to\frac{N!}{k_{m_0}!}\pi_{k_{m_0}}^{k_{m_0}}(C_{m_0})g_{k_{m_0},k_{m_0+1}}(\omega_{k_{m_0+1}};C_{m_0})$$

it is possible to repeat the calculation exactly in the same way and finally get

$$P\left(\bigcap_{m=m_0}^{M}\mathcal{A}(k_m,C_m)\right)=\frac{N!}{k_{m_0}!}\pi_{k_{m_0}}^{k_{m_0}}(C_{m_0})\prod_{m=m_0}^{M}g_{k_m,k_{m+1}+1}(\pi_{k_{m+1}+1}(C_{m+1});C_m).$$

Here $k_{M+1}=N, \pi_{N+1}=1$.

Substitution of this result to (14) leads to

$$P_{(k_0,C_0)|(k_1,C_1),\ldots,(k_M,C_M)}=\frac{k_1!}{k_0!}\frac{\pi_{k_0}^{k_0}(C_0)}{\pi_{k_1}^{k_1}(C_1)}g_{k_0,k_1+1}(\pi_{k_1+1}(C_1);C_0)=P_{(k_0,C_0)|(k_1,C_1)}.$$

Surprisingly, the conditional probability depends only on the last observed state of the well. Probably, there exist a more elegant (than direct calculation presented here) way to prove this fact.

---

[1] M. Ahsanullah, V. B. Nevzorov, and M. Shakil. *An Introduction to Order Statistics, Atlantis Studies in Probability and Statistics 3.* Atlantis Press, 2013.

[2] R. Baldick, B. Chowdhury, I. Dobson, Z. Dong, B. Gou, D. Hawkins, H. Huang, M. Joung, D. Kirschen, F. Li, J. Li, Z. Li, C. C. Liu, L. Mili, S. Miller, R. Podmore, K. Schneider, K. Sun, D. Wang, Z. Wu, P. Zhang, W. Zhang, and X. Zhang. Initial review of methods for cascading failure analysis in electric power transmission systems. In *IEEE Power and Energy Society*

2008 General Meeting: Conversion and Delivery of Electrical Energy in the 21st Century, PES, 2008.

[3] R. Bellman. A Markovian decision process. *Journal of Mathematics and Mechanics*, pages 679–684, 1957.

[4] A. V. Brovchuk, I. Diyashev, A. V. Lipyanin, D. Grant, D. Oussoltsev, and K. K. Butula. Fracturing Treatments of Openhole Horizontal Wells in Western Siberia (Russian). In *SPE Russian Oil and Gas Technical Conference and Exhibition (SPE-102417-RU)*, page 19, Moscow, Russia, 2006. Society of Petroleum Engineers.

[5] A Ali Daneshy. Hydraulic Fracturing of Horizontal Wells: Issues and Insights, 2011.

[6] M.J. Economides and K.G. Nolte. *Reservoir Stimulation, Third Edition.* John Wiley & Sons, 2000.

[7] Hengdao Guo, Ciyan Zheng, Herbert Ho Ching Iu, and Tyrone Fernando. A critical review of cascading failure analysis and modeling of power system, 2017.

[8] R. A. Howard. *Dynamic programming and Markov processes.* John Wiley, 1960.

[9] E. Isaacson and H.B. Keller. *Analysis of numerical methods.* Dover, 1994.

[10] A. A. Osiptsov, E. Zilonova, S. Boronin, J. Desroches, N. Lebedeva, and D. Willberg. Insights on overflushing strategies from a novel modeling approach to displacement of yield-stress fluids in a fracture. 01 2016.

[11] M. L. Puterman. *Markov decision processes: discrete stochastic dynamic programming.* John Wiley & Sons, 1994.

[12] R. Sachdeva, Z. Schmidt, J.P. Brill, and R.M. Blais. Two-Phase Flow Through Chokes. *Proceedings of SPE Annual Technical Conference and Exhibition*, October 1986.

[13] Jiajia Song, Eduardo Cotilla-Sanchez, Goodarz Ghanavati, and Paul D.H. Hines. Dynamic modeling of cascading failure in power systems. *IEEE Transactions on Power Systems*, 2016.

[14] P.E. Spesivtsev, A.D. Kharlashkin, and K.F. Sinkov. Study of the transient terrain-induced and severe slugging problems by use of the drift-flux model. *SPE Journal*, (SPE-186105-PA), 2017.

[15] Milorad Stanojcic, Omkar A Jaripatke, and Amit Sharma. Pinpoint Fracturing Technologies: A Review of Successful Evolution of Multistage Fracturing in the Last Decade, 2010.

[16] Mike C Vincent. Optimizing Transverse Fractures in Liquid-Rich Formations, 2011.

[17] S. Whitaker. Flow in porous media I: A theoretical derivation of Darcy's law. *Transport in*

Porous Media, 1:3–25, 1986.

[18] Wikipedia contributors. Cascading failure — Wikipedia, the free encyclopedia, 2019. [Online; accessed 11-October-2019].